

Diversity over Uniformity: Rethinking Representation in Generated Image Detection

Qinghui He^{1,2}, Haifeng Zhang^{1,2}, Qiao Qin^{1,2}, Bo Liu^{1,3}*, Xiuli Bi^{1,3}, Bin Xiao^{1,4}

¹Chongqing Key Laboratory of Image Cognition

Chongqing University of Posts and Telecommunications, Chongqing, China

²School of Computer Science and Technology ³School of Artificial Intelligence

⁴Jinan Inspur Data Technology Co., Ltd., Jinan, China

{D250201011, D240201065, S240201048}@stu.cqupt.edu.cn

{boliu, bixl, xiaobin}@cqupt.edu.cn

Abstract

With the rapid advancement of generative models, generated image detection has become an important task in visual forensics. Although existing methods have achieved remarkable progress, they often rely, after training, on only a small subset of highly salient forgery cues, which limits their ability to generalize to unseen generative mechanisms. We argue that reliably generated image detection should not depend on a single decision path but should preserve multiple judgment perspectives, enabling the model to understand the differences between real and generated images from diverse viewpoints. Based on this idea, we propose an anti-feature-collapse learning framework that filters task-irrelevant components and suppresses excessive overlap among different forgery cues in the representation space, preventing discriminative information from collapsing into a few dominant feature directions. This design maintains diverse and complementary evidence within the model, reduces reliance on a small set of salient cues, and enhances robustness under unseen generative settings. Extensive experiments on multiple public benchmarks demonstrate that the proposed method significantly outperforms the state-of-the-art approaches in cross-model scenarios, achieving an accuracy improvement of 5.02% and exhibiting superior generalization and detection reliability. The source code is available at <https://github.com/Yanmou-Hui/DoU>.

1. Introduction

With the rapid progress of generative models such as GANs and diffusion models, AI-generated images have achieved a level of realism that often surpasses human perception.

* Corresponding Author

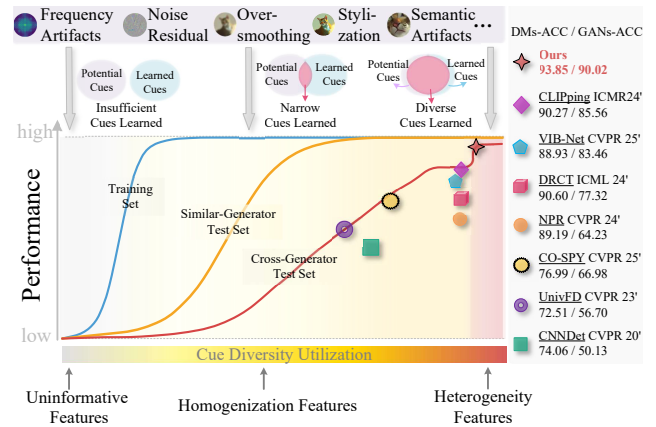


Figure 1. Conceptual illustration and empirical comparison of feature utilization in generated image detection. The limitation of existing detectors lies not in the lack of features, but in relying only on the most salient cues. Our method learns diverse discriminative features, maintaining representational heterogeneity.

These models can produce high-quality, semantically consistent images across diverse domains, resulting in the widespread circulation of synthetic media in social and news platforms. While this advancement has benefited creative industries, it also raises serious concerns about misinformation and visual authenticity. As a result, distinguishing real images from generated ones has become a core problem in visual forensics. The goal is to reliably identify AI-generated images under unknown or concealed generation mechanisms, making the development of robust and generalizable detection methods crucial for ensuring content authenticity and supporting applications such as media verification and digital forensics.

A more subtle challenge in current generated image detection does not lie in the insufficiency of features, but in the

tendency of models to compress multi-source information into similar discriminative patterns during training, exhibiting a pronounced representational homogenization. Deep models often prioritize learning the most salient and easily distinguishable artifacts for real-fake separation, and establish stable decision boundaries based on these cues. This learning behavior gradually narrows the feature space, weakening the diversity among discriminative dimensions and leading to highly similar internal representations. Although such convergence facilitates fast optimization and yields good performance under specific generation models or data distributions, it causes the model to rely excessively on fixed discriminative cues, thereby reducing its ability to adapt to diverse generative techniques. When the generation method, image content, or perturbation type changes, the model, lacking multi-source and complementary features, struggles to adapt its decision criteria to new generative techniques, resulting in a significant degradation of detection performance.

To address this issue, we propose a novel research perspective: reliably generated image detection should not rely on a single discriminative path but should preserve multiple judgment perspectives. We aim to maintain diverse discriminative representations within the model, enabling it to understand the differences between real and generated images from multiple viewpoints rather than being dominated by a single decision pattern. Such representational heterogeneity acts as a resistance mechanism against the convergence of feature homogenization, ensuring the coexistence of multiple independent and complementary discriminative cues within the model. This design reduces reliance on specific artifacts and enhances the model’s robustness when facing shifts in generative techniques, content domains, or unknown perturbations. Based on this concept, we propose an Anti-Feature-Collapse Learning (AFCL) method, which explicitly encourages representational heterogeneity and complementarity during training to suppress feature homogenization and maintain the openness and diversity of the discriminative space. The performance improvement achieved by AFCL does not come from an increase in information quantity, but from the preservation of diverse discriminative perspectives. Furthermore, we introduce a theoretical constraint mechanism to ensure that the model captures sufficient forgery-related cues while removing task-irrelevant redundant features, thereby strengthening its discriminative capability.

To validate the effectiveness of the proposed method, we conduct extensive experiments on multiple public benchmarks for generated image detection, covering a wide range of generative architectures based on both GANs and diffusion models. The experimental results demonstrate that the proposed approach significantly outperforms existing detection methods in cross-model and unseen-generator

scenarios. The proposed anti-feature-collapse mechanism effectively maintains representational diversity, enhancing the model’s robustness and generalization capability under complex generation patterns. The main contributions are summarized as follows:

- We propose a novel generated image detection method named AFCL, which explicitly encourages internal representational heterogeneity and complementarity during training, effectively mitigating the trend of feature homogenization and providing richer and more generalizable forgery cues for reliable discrimination.
- We introduce a theoretical constraint to ensure that the model extracts sufficient forgery-related features, thereby removing redundant information and enhancing task-specific discriminability.
- Extensive experiments on multiple public benchmarks for generated image detection show that our method consistently outperforms existing state-of-the-art methods, demonstrating the effectiveness of anti-feature-collapse learning in improving robustness and generalization.

2. Related Works

2.1. Feature-Driven Generated Image Detection

The rapid development of generative networks has spurred extensive research on generated image detection. Most existing approaches focus on learning one or several discriminative forgery features to distinguish real images from generated ones. Early studies are often effective only within a specific generative paradigm (such as GANs). Wang et al. [39] use a simple CNN classifier with data augmentation to detect unseen GAN-generated images. [5, 14, 16, 25] reveal that GAN-generated images differ significantly from real ones in the frequency domain. Chandrasegaran et al. [6] identify color information as a transferable cue for cross-model detection, while Jia et al. [21] observe that generated images exhibit higher color saturation and uneven distributions, and propose color quantization and recovery-based features for detection. Tan et al. [36] find that the gradient information from pretrained models can serve as a general artifact for detection. In addition, they introduce NPR [37] to capture local up-sampling artifacts. Corvi et al. [11] demonstrate that existing detectors trained on GANs generalize poorly to diffusion models, motivating diffusion-specific designs. Wang et al. [40] propose using reconstruction errors from diffusion models for detection, while Cazenavette et al. [4] leverage the inversion of pretrained Stable Diffusion to obtain latent noise and reconstructed images as auxiliary discriminative representations. Luo et al. [26] compute single-step latent reconstruction errors for efficiency, and Ricker et al. [32] achieve training-free detection via autoencoder reconstruction errors. Chu et al. [10] reveal that diffusion models inadequately recon-

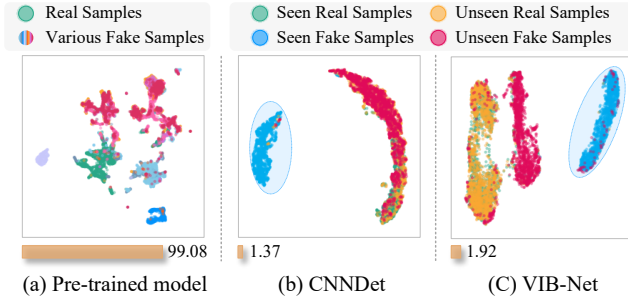


Figure 2. **UMAP visualizations with effective-rank bars.** (a) Features of real and various generated samples extracted by a pre-trained model. (b) CNNDet and (c) VIB-Net features on seen and unseen samples. Bars denote the effective rank. A higher value reflects more diverse and evenly distributed feature representations, whereas a lower rank implies feature collapse and reliance on a few dominant cues.

struct mid-frequency components of real images and integrated frequency decomposition with reconstruction-error modeling to extract more discriminative features. Meanwhile, DRCT [7], Bias-Free [18], and SFLD [19] decouple content- and artifact-related representations, constructing bias-free datasets through diffusion-based reconstruction to reduce overfitting to semantic content. These studies provide important insights into detecting GAN- or diffusion-generated images, but still struggle to achieve cross-model generalization.

2.2. Generalizable Generated Image Detection

To address the challenge of cross-model generalization, recent studies have begun exploring unified detection frameworks based on pretrained multimodal models. Specifically, Ojha et al. [28] leverage the pretrained CLIP [30] feature space and perform linear fine-tuning, thereby significantly enhancing the detector’s generalization across different generative models. Cozzolino et al. [12] observe that CLIP features capture high-level semantic artifacts rather than low-level frequency cues. Khan et al. [24] combine CLIP’s visual and textual branches and adopt prompt tuning, achieving notable improvements in generalization. Wu et al. [41] formulate generated image detection as a few-shot classification problem and employ prototype-based metric learning to enable efficient detection with very limited samples from unseen generators. Zhang et al. [44] introduce a variational information bottleneck mechanism into multimodal features, explicitly compressing task-irrelevant information while preserving the features most relevant to real-fake discrimination.

3. Empirical Motivation and Analysis

To investigate the root cause of the limited generalization ability of existing detectors, we first visualize the feature

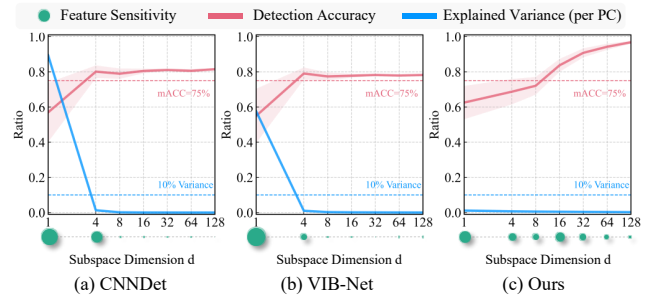


Figure 3. **Subspace-based evaluation with explained variance analysis.** The green circles denote *feature sensitivity*, where a larger circle indicates higher sensitivity to the corresponding principal component. The red line shows the detection accuracy (mACC) achieved when using different subspace dimensions. The blue line represents the *information contribution* of each principal component (by PCA), reflecting its relative importance to the overall feature representation.

distributions of different models, as shown in Fig. 2. The features extracted by a pre-trained model form a broad and uniformly distributed structure between real and generated samples, indicating that those features retain a rich diversity of discriminative cues. As shown in Fig. 2(b)(c), both CNNDet and VIB-Net exhibit clear generalization failures. These detectors tend to misclassify generated samples that do not share forgery patterns similar to those seen in the training set as real. Although unseen generated samples still exhibit subtle discrepancies compared to real ones, these relatively weak discriminative features are not effectively exploited by the models, resulting in generalization failure. Meanwhile, we observe that these detectors have a significantly reduced effective rank, further revealing their strong reliance on a few dominant feature directions. This phenomenon suggests that the fundamental limitation of current detectors does not lie in the insufficiency of discriminative features, but rather in the way these features are organized and utilized within the model. During training, detectors tend to converge toward the most salient and easily learnable discriminative cues, forming a dominant and shortcut-like decision pattern [28, 43]. As training progresses, the model gradually compresses forgery evidence from multiple sources into a single discriminative subspace, thereby losing representational diversity and weakening its adaptability to unseen generative mechanisms.

To further verify this observation, we conduct a subspace-based analysis. As illustrated in Fig. 2(a)(b), both CNN-based and ViT-based detectors exhibit similar feature contraction behavior. Their detection performance rapidly saturates with only a few principal components, and adding more components brings almost no further improvement, suggesting that most discriminative capacity is concentrated in a few feature directions. The blue curve indi-

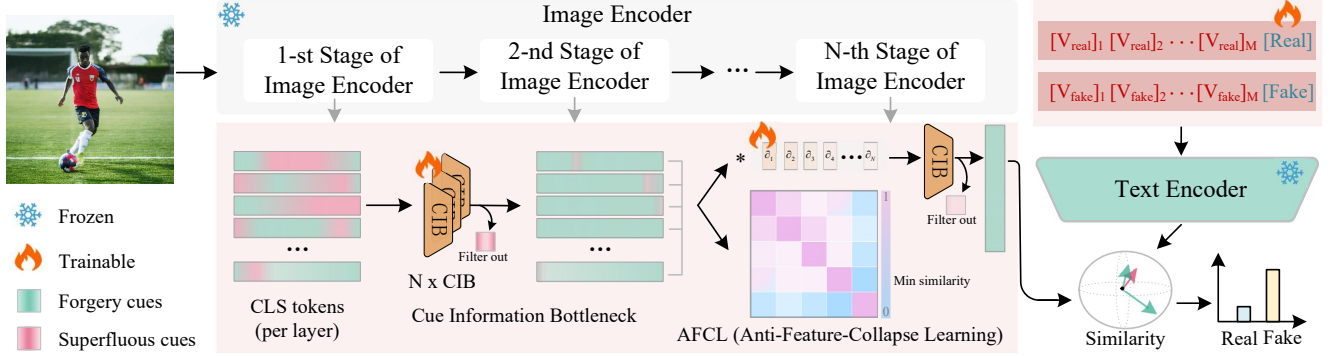


Figure 4. Overview of our proposed AFCL framework. The frozen image encoder provides multi-stage CLS embeddings, which are refined by the CIBs to remove superfluous cues. AFCL enforces layer-wise decorrelation to maintain feature diversity. The resulting representations are aligned with real/fake textual embeddings for classification.

icates that a large portion of feature variance remains underutilized, while the rapid saturation of the performance curve (highlighted in green) reveals the model’s high sensitivity to specific components, reflecting the fragility of the decision boundary and the dependency of the representation. This observation further indicates that existing detectors implicitly integrate heterogeneous forgery cues into a single dominant direction during optimization, causing the feature space to collapse from a diverse, multi-cue structure into a narrow sub-manifold. Although this sub-manifold maximizes separability, it sacrifices orthogonal information and robustness. Once the key discriminative features shift or disappear in new generative samples, the detector’s decision foundation collapses, leading to a significant drop in generalization performance.

Based on the above findings, we further design a validation experiment by explicitly introducing a representational heterogeneity constraint during training to encourage the learning of diverse forgery cues. As shown in Fig. 2(c), after incorporating this constraint, the detector’s accuracy gradually improves with increasing subspace dimensionality, instead of saturating within only a few principal components. This demonstrates that the model can effectively utilize multiple complementary cues, making its decision process less sensitive to specific components and enabling more comprehensive exploitation of overall feature information. These results validate our hypothesis and indicate that, to maintain reliable decision-making under distributional shifts, detectors need to preserve diverse and complementary discriminative representations.

4. Method

4.1. Overview

The proposed framework aims to improve the generalization capability of generated image detectors by addressing two essential aspects of representation learning: eliminat-

ing irrelevant and spurious features, and preserving heterogeneous and complementary discriminative cues. As illustrated in Fig. 4, given an input image, a pretrained and frozen image encoder produces multi-stage CLS representations that capture hierarchical and complementary forgery cues. Each stage feature is first refined by the Cue Information Bottleneck (CIB) module, which preserves task-relevant signals and removes redundant correlations that do not contribute to authenticity discrimination. To maintain diversity across stages, the Anti-Feature-Collapse Learning (AFCL) module imposes an inter-stage decorrelation constraint, encouraging each layer to capture distinct aspects of forgery evidence. The stage-wise features are then aggregated through learnable weights to adaptively balance contributions from different representation levels, followed by another CIB refinement to suppress residual noise. Finally, the aggregated representation is aligned with learnable textual prototypes of “real” and “fake” through cosine similarity to produce the final prediction.

4.2. Cue Information Bottleneck

The CIB module is designed to refine multiple forgery cues by explicitly filtering out superfluous cues. Formally, given an input image x and its authenticity label $y \in \{0, 1\}$, the frozen image encoder produces multi-stage CLS features:

$$\mathcal{V} = \{v_1, v_2, \dots, v_N\}, \quad v_i \in \mathbb{R}^D, \quad (1)$$

where v_i denotes the feature of the i -th stage. Each v_i passes through an independent learnable transformation module $\text{CIB}(\cdot)$ that performs information filtering:

$$\tilde{v}_i = \text{CIB}_i(v_i), \quad \tilde{\mathcal{V}} = \{\tilde{v}_1, \tilde{v}_2, \dots, \tilde{v}_N\}. \quad (2)$$

where each \tilde{v}_i encodes one aspect of potential forgery cue. The objective of CIB is to maximize predictive relevance between each purified cue \tilde{v}_i and the label y , while minimizing the dependency between \tilde{v}_i and the input x :

$$\max_{\{\text{CIB}_i\}} \sum_{i=1}^N [I(\tilde{v}_i; y) - \beta I(\tilde{v}_i; x)], \quad (3)$$

where $I(\cdot, \cdot)$ denotes mutual information and $\beta > 0$ controls the compression strength. The first term ensures comprehensiveness by retaining discriminative authenticity-related cues, while the second term enforces compactness by suppressing task-independent variations. To better interpret the contribution of different cues, we reformulate the joint objective as:

$$I(y; \tilde{\mathcal{V}}) = \sum_{i=1}^N I(y; \tilde{v}_i | \tilde{\mathcal{V}} \setminus \tilde{v}_i), \quad (4)$$

which indicates that each cue contributes distinct evidence for real-fake discrimination conditioned on others.

For tractable optimization, we derive a variational lower bound based on the Kullback–Leibler divergence:

$$I(y; \tilde{v}_i | \tilde{\mathcal{V}} \setminus \tilde{v}_i) \geq \text{D}_{\text{KL}}[p(y | \tilde{\mathcal{V}} \setminus \tilde{v}_i) || p(y | \tilde{\mathcal{V}})], \quad (5)$$

leading to the empirical CIB loss:

$$\mathcal{L}_{\text{CIB}} = \sum_{i=1}^N \text{D}_{\text{KL}}[p(y | \tilde{\mathcal{V}}) || p(y | \tilde{\mathcal{V}} \setminus \tilde{v}_i)]. \quad (6)$$

Minimizing \mathcal{L}_{CIB} encourages each cue \tilde{v}_i to carry essential information for authenticity discrimination, forming a set of purified and complementary features $\tilde{\mathcal{V}}$.

4.3. Anti-Feature-Collapse Learning

While the CIB purifies task-relevant cues within each representation, it does not explicitly regulate the relationships among different cues. As training proceeds, deep detectors tend to converge toward a few dominant discriminative cues, leading to increasingly correlated representations and a loss of diversity. This phenomenon, referred to as feature collapse, causes the detector to rely excessively on the most salient pattern and severely limits its generalization to unseen generative models.

To alleviate this issue, we introduce AFCL, which maintains structural diversity among cue representations by enforcing decorrelation. Given the refined set of characteristics $\tilde{\mathcal{V}} = \{\tilde{v}_1, \tilde{v}_2, \dots, \tilde{v}_N\}$, each \tilde{v}_i encodes a different type of forgery evidence. AFCL measures the dependency between any two cue features using the Hilbert–Schmidt Independence Criterion (HSIC), a kernel-based dependence metric that equals zero if and only if the variables are independent. For two representations \tilde{v}_i and \tilde{v}_j , the empirical HSIC is computed as:

$$\text{HSIC}(\tilde{v}_i, \tilde{v}_j) = \frac{1}{(B-1)^2} \text{Tr}(K_i H K_j H), \quad (7)$$

where K_i and K_j are the Gram matrices of the features, H is the centering matrix, and B denotes the batch size. The overall AFCL objective averages pairwise dependencies across all cues:

$$\mathcal{L}_{\text{AFCL}} = \frac{1}{N(N-1)} \sum_{i \neq j} \text{HSIC}(\tilde{v}_i, \tilde{v}_j), \quad (8)$$

Minimizing $\mathcal{L}_{\text{AFCL}}$ encourages representational independence, ensuring that different cues retain complementary and orthogonal discriminative properties.

Once diversity is enforced, AFCL adaptively integrates the decorrelated cues through a learnable weighted aggregation:

$$v_{\text{agg}} = \sum_i^N \alpha_i \tilde{v}_i, \quad \text{where } \sum_i \alpha_i = 1, \quad \alpha_i \geq 0. \quad (9)$$

The weights α_i are optimized jointly with the network, allowing the detector to automatically balance contributions from heterogeneous cues. To prevent weight collapse, we introduce a weight uniformity regularization that encourages a more balanced distribution:

$$\mathcal{L}_{\text{reg}} = \left(\sum_{i=1}^N \alpha_i^2 - \frac{1}{N} \right)^2, \quad (10)$$

This regularization term attains its minimum when all cues contribute equally, avoiding over-dependence on a small subset of features. The final aggregated representation is further refined by a global CIB module:

$$\tilde{v}_{\text{final}} = \text{CIB}(v_{\text{agg}}). \quad (11)$$

which suppresses residual noise and reinforces authenticity-related information.

4.4. Class-Specific Prompt Learning

We adopt a Class-Specific Prompt Learning (CSP) strategy that dynamically aligns visual representations with category-aware textual concepts inspired by CoOp [45]. Instead of relying on fixed textual templates (e.g., “a photo of a real image”), CSP parameterizes the textual prompts for each authenticity category as a sequence of learnable context vectors:

$$T_c = [T_c^1, T_c^2, \dots, T_c^M, [C]], \quad (12)$$

where T_c^m denotes the m -th learnable token and $[C]$ is the class token corresponding to “real” or “fake”. Each prompt T_c is encoded by the frozen CLIP text encoder to obtain the prototype $e_c = f_{\text{text}}(T_c)$. The final image feature \tilde{v}_{final} is projected into the shared visual-semantic space, and authenticity is determined by cosine similarity:

$$s_c = \frac{\tilde{v}_{\text{final}} \cdot e_c}{\|\tilde{v}_{\text{final}}\| \|e_c\|}, \quad c \in \{\text{real}, \text{fake}\}. \quad (13)$$

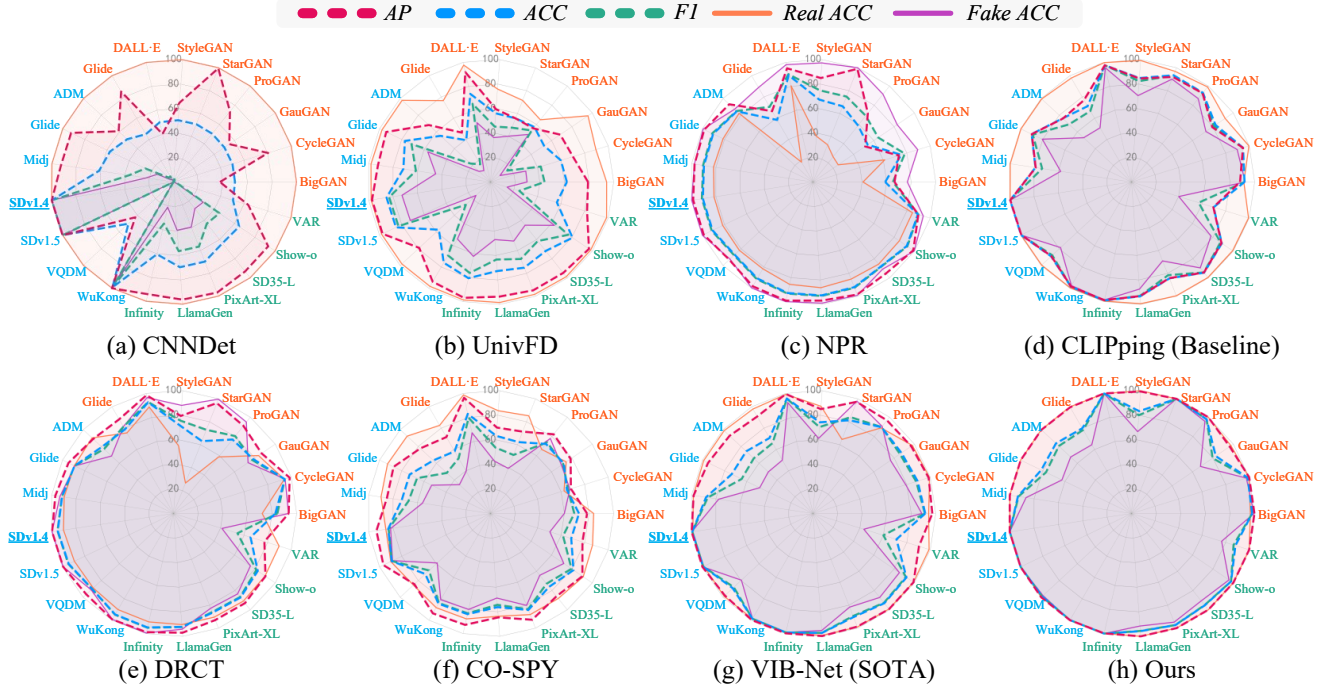


Figure 5. **Cross-model generalization comparison on multiple generative sources.** All detectors are trained on SD v1.4 and evaluated on representative subsets from UniversalFakeDetect, GenImage, and AIGI-Holmes. The radar plots report the performance across 21 generative models in terms of *AP*, *ACC*, *FI*, *Real ACC*, and *Fake ACC*.

Then, the similarity scores are normalized with a softmax function to produce class probabilities:

$$p_c = \frac{\exp(s_c/\tau)}{\sum_{c'} \exp(s_{c'}/\tau)}, \quad (14)$$

Finally, the class-specific prompts are optimized using a cross-entropy loss:

$$\mathcal{L}_{\text{CSP}} = - \sum_{c \in \{\text{real}, \text{fakke}\}} y_c \log(p_c), \quad (15)$$

where y_c is the one-hot label indicating the ground-truth authenticity.

4.5. Optimization Objective

All modules are jointly optimized in an end-to-end manner under a unified objective that integrates cue purification, diversity preservation, aggregation regularization, and authenticity alignment. The total training loss is formulated as:

$$\mathcal{L} = \mathcal{L}_{\text{CSP}} + \lambda_1 \mathcal{L}_{\text{CIB}} + \lambda_2 \mathcal{L}_{\text{AFCL}} + \lambda_3 \mathcal{L}_{\text{reg}}. \quad (16)$$

where λ_1 , λ_2 , and λ_3 control the relative contributions of the respective terms. This joint objective drives the detector to build a compact yet heterogeneous authenticity-aware representation space, where purified, diversified, and balanced cues collectively support robust generalization to unseen generative mechanisms.

5. Experiments

In this section, we first introduce the experimental setup, including datasets, evaluation metrics, and implementation details. We then present a comprehensive comparison between our method and state-of-the-art methods. Furthermore, we conduct ablation studies to analyze the contribution of each component, and perform robustness experiments to evaluate the model’s stability.

5.1. Experimental Setup

Training dataset. We use the Stable Diffusion v1.4 subset of the GenImage [48] to ensure a fair and consistent comparison with previous works. The dataset contains a large number of real and generated image pairs across diverse scenes and categories, providing a comprehensive benchmark for evaluating generated image detectors.

Testing dataset. To comprehensively evaluate the detection capability of our method in real-world scenarios, we conduct experiments on three large-scale benchmarks: UniversalFakeDetect [28], GenImage [48], and AIGI-Holmes [46]. These benchmarks jointly cover both GAN- and diffusion-based paradigms, with a wide range of resolutions, semantics, and generation styles.

Specifically, we select 11 mainstream subsets including BigGAN [3], CycleGAN [47], GauGAN [29], ProGAN [22], StarGAN [9], StyleGAN [23], DeepFakes [34],

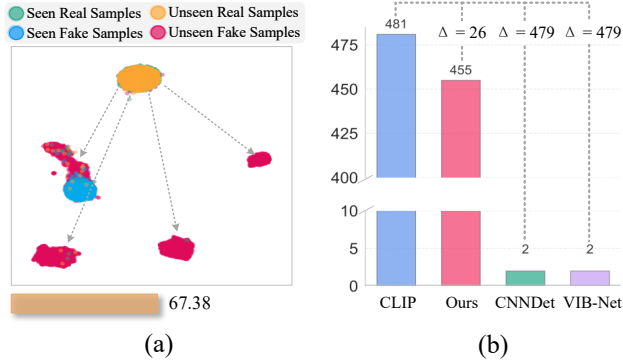


Figure 6. (a) UMAP visualizations with effective-rank bars. (b) Comparison of the number of PCA components needed by each detector to account for 90% of the total variance (PCs@90%).

Guided Diffusion [13], LDM [33], GLIDE [27], and DALL-E [31] from *UniversalFakeDetect*. *GenImage* primarily focuses on diffusion-based models, including ADM [13], GLIDE [27], Midjourney [1], SD v1.4 and SD v1.5 [33], VQDM [17], and Wukong [2]. *AIGI-Holmes* comprises high-resolution diffusion-generated images and compressed, web-scraped real images. It includes subsets generated by recent diffusion models, such as Infinity [20], LlamaGen [35], PixArt-XL [8], SD3.5-L [15], Show-o [42], and VAR [38].

Evaluation metrics. Following prior works [25, 39, 44], we adopt average precision (AP) and classification accuracy (ACC) as the primary evaluation metrics. To assess potential bias, we also report *F1* scores, as well as real-image accuracy (*Real ACC*) and generated-image accuracy (*Fake ACC*) in some experiments.

Implementation details. All experiments are implemented in PyTorch and trained on NVIDIA H100 PCIe GPUs. We use the Adam optimizer with an initial learning rate of 1×10^{-4} and a batch size of 512 with early stopping applied to prevent overfitting. The CLIP:ViT-L/14 model serves as the backbone for feature extraction, and we apply the same data augmentation strategy as described in [44].

5.2. Comparisons of Detection Performance

In this section, we compare the detection performance of our method with a series of state-of-the-art generated image detection approaches across multiple benchmark datasets. For fairness, all models are trained on the same SD v1.4 subset and evaluated under identical experimental settings.

As shown in Fig. 5, traditional detectors such as CNNDet [39] and UnivFD [28] achieve strong detection accuracy when the testing data share similar generation characteristics with the training set. However, their performance drops significantly on unseen domains, particularly on GAN-generated or high-resolution diffusion-generated images, revealing their strong dependence on source-specific

CIB	AFCL	reg	ACC		AP	
			avg	cross	avg	cross
×	×	×	87.81%	85.56%	87.32%	84.69%
✓	×	✓	89.72%	85.99%	99.38%	98.73%
×	✓	✓	91.60%	91.15%	99.40%	98.73%
✓	✓	✓	92.81%	90.02%	99.52%	98.90%

Table 1. Ablation study on the contributions of the components. “×” indicates the component is disabled, while “✓” indicates it is enabled. avg denotes the average over all test sets, while cross denotes the average over cross-generator evaluations.

artifacts. Methods such as NPR [37] and CO-SPY [21] rely heavily on a small set of discriminative cues. These cues generalize moderately across visually similar generators but fail when the generation paradigm differs substantially, such as in the case of GAN-based images. More advanced methods, including CLIPping [24], DRCT [7], and VIB-Net [44], improve generalization by explicitly reducing data bias and suppressing spurious correlations during training, which alleviates overfitting to specific generation biases. Nevertheless, their performance remains inconsistent across benchmarks, suggesting that debiasing alone is insufficient to achieve stable generalization.

In contrast, our method achieves high and balanced performance across all generative sources. On average, it attains 99.52% AP and 92.81% ACC, surpassing the state-of-the-art method (VIB-Net) by 3.39% AP and 5.68% ACC, and outperforming the baseline (CLIPping) by 12.20% AP and 5.00% ACC. These results validate the effectiveness of our design in maintaining diverse and complementary representations, leading to superior cross-model generalization and reliable detection performance.

5.3. Representation Diversity Analysis

To better understand how our method shapes the feature space, we examine the structure of the learned representations by visualizing their distribution and measuring their effective rank. As shown in Fig. 6(a), our method maintains clear separability between real and generated images and simultaneously preserves the diversity among distinct generative sources. The corresponding effective rank reaches 67.38, reflecting a more evenly distributed and heterogeneous representation manifold. In contrast, CNNDet and VIB-Net in Fig. 2 exhibit severely compressed manifolds with effective ranks of only 1.37 and 1.92. Fig. 6(b) provides a quantitative evaluation through the number of principal components required to explain 90% of the variance (PCs@90%). Existing detectors greatly compress the representational space of the pretrained backbone, often eliminating hundreds of meaningful feature directions. Our

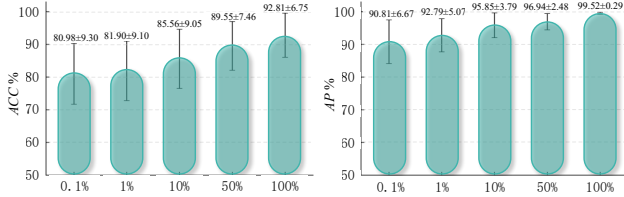


Figure 7. **Few-shot performance for generated image detection.** The bar chart reports *ACC* and *AP* under varying training data ratios (0.1%, 1%, 10%, 50%, 100%). Both metrics steadily improve as more training data becomes available.

method preserves the majority of the original representational structure, reducing only 26 principal components. This observation demonstrates that maintaining a high-rank, diverse feature space enables the detector to retain pre-trained knowledge more effectively and to generalize more effectively to unseen generative mechanisms.

5.4. Ablation Study

To evaluate the contributions of each component, we conduct an ablation study summarized in Table 1. Adding CIB yields a clear improvement over the baseline, increasing the average accuracy from 87.81% to 89.72% and the average *AP* from 87.32% to 99.38%, indicating that removing superfluous information effectively strengthens task-relevant cues. Introducing AFCL leads to further gains, particularly in cross-model accuracy, which rises from 85.56% to 91.15%, showing that maintaining diverse and complementary cues improves robustness to distribution shifts. When all components are combined, the model achieves the best performance, reaching 92.81% average accuracy and 99.52% average *AP*. These results demonstrate that information purification and anti-collapse learning work synergistically to enhance both overall and cross-model generalization.

5.5. Few-shot Performance

To assess the data efficiency of our method, we train the detector using different proportions of the full dataset: 0.1% (320 samples), 1% (3.2k), 10% (32k), 50% (160k), and 100% (320k). As shown in Fig. 7, our method achieves strong performance even under extremely limited supervision—for example, using only 0.1% of the data, it already obtains 80.98% *ACC* and 90.81% *AP*. As more data becomes available, both metrics improve steadily, reaching 92.81% *ACC* and 99.52% *AP* with the full dataset. These results demonstrate that our framework maintains high sample efficiency, achieving competitive performance even with very limited data, and continues to improve steadily as more training samples are provided, showing a strong ability to make effective use of supervision at all scales and to adapt to richer training signals.

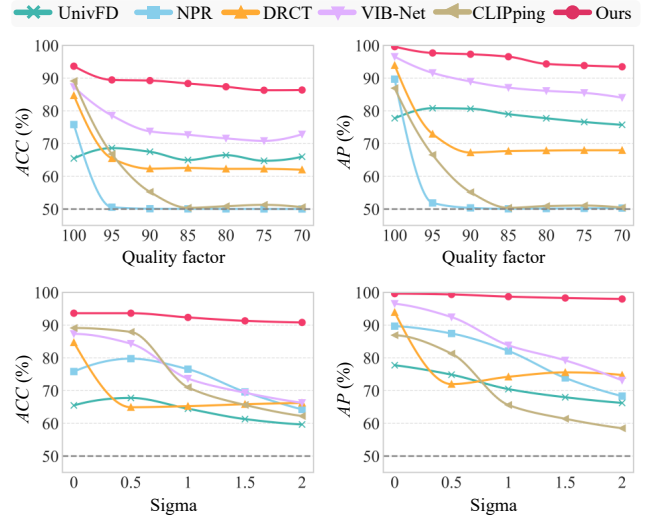


Figure 8. **Robustness evaluation under perturbations.** The top row shows performance under different JPEG compression quality factors, while the bottom row reports results under Gaussian blur with increasing sigma. Both *ACC* and *AP* are presented for each method, providing a comprehensive comparison of robustness against common post-processing distortions.

5.6. Robustness to Unseen Perturbations

In real-world scenarios, images are frequently affected by various post-processing operations, making robustness to perturbations an essential aspect of evaluating detector reliability. We therefore assess performance under two commonly encountered distortions, JPEG compression and Gaussian blur, as shown in Fig. 8. As the perturbation strength increases, different detectors exhibit varying levels of sensitivity to degraded inputs. Methods that depend more heavily on localized or high-frequency artifacts tend to show larger decreases in performance, while approaches with stronger feature abstraction generally retain better stability. Overall, accuracy declines are observed to varying degrees across existing baselines as distortions intensify. Our method maintains the highest *ACC* and *AP* across all distortion levels in both settings. This robustness arises from the proposed attribution-focused feature modeling, which captures stable cross-cue evidence and reduces reliance on pixel-level details that are easily altered by post-processing operations.

6. Conclusion

In this work, we revisit the core challenges of generalization in generated image detection and identify a fundamental limitation of existing detectors: during training, diverse forgery cues often collapse into a small set of dominant feature directions, leading to brittle decision boundaries and poor adaptation to unseen generative models. To address this issue, we introduce a unified detec-

tion framework that combines cue-level information purification, inter-cue diversity preservation, and class-specific authenticity modeling. Together, these components maintain heterogeneous and complementary sources of evidence, suppress spurious or redundant patterns, and construct a well-structured, authenticity-aware feature space. Extensive experiments across multiple benchmarks demonstrate that preserving diverse and high-rank representations is critical for achieving robust cross-model generalization.

References

- [1] Midjourney., 2022. 2023 in <https://www.midjourney.com>. 7
- [2] wukong, 2022. 2022.5 in <https://xihe.mindsore.cn/>. 7
- [3] Andrew Brock, Jeff Donahue, and Karen Simonyan. Large scale gan training for high fidelity natural image synthesis. In *International Conference on Learning Representations*, 2018. 6
- [4] George Cazenavette, Avneesh Sud, Thomas Leung, and Ben Usman. Fakeinversion: Learning to detect images from unseen text-to-image models by inverting stable diffusion. In *Proceedings of the IEEE/CVF Conference on Computer Vision and Pattern Recognition*, pages 10759–10769, 2024. 2
- [5] Keshigeyan Chandrasegaran, Ngoc-Trung Tran, and Ngai-Man Cheung. A closer look at fourier spectrum discrepancies for cnn-generated images detection. In *Proceedings of the IEEE/CVF conference on computer vision and pattern recognition*, pages 7200–7209, 2021. 2
- [6] Keshigeyan Chandrasegaran, Ngoc-Trung Tran, Alexander Binder, and Ngai-Man Cheung. Discovering transferable forensic features for cnn-generated images detection. In *European Conference on Computer Vision*, pages 671–689. Springer, 2022. 2
- [7] Baoying Chen, Jishen Zeng, Jianquan Yang, and Rui Yang. Drc: Diffusion reconstruction contrastive training towards universal detection of diffusion generated images. In *Forty-first International Conference on Machine Learning*, 2024. 3, 7
- [8] J Chen, C Ge, E Xie, Y Wu, L Yao, X Ren, Z Wang, P Luo, H Lu, and Z Pixart Li. Weak-to-strong training of diffusion transformer for 4k text-to-image generation. In *European Conference on Computer Vision*, pages 74–91, 2024. 7
- [9] Yunjey Choi, Minje Choi, Munyoung Kim, Jung-Woo Ha, Sunghun Kim, and Jaegul Choo. Stargan: Unified generative adversarial networks for multi-domain image-to-image translation. In *Proceedings of the IEEE conference on computer vision and pattern recognition*, pages 8789–8797, 2018. 6
- [10] Beilin Chu, Xuan Xu, Xin Wang, Yufei Zhang, Weike You, and Linna Zhou. Fire: Robust detection of diffusion-generated images via frequency-guided reconstruction error. In *Proceedings of the Computer Vision and Pattern Recognition Conference*, pages 12830–12839, 2025. 2
- [11] Riccardo Corvi, Davide Cozzolino, Giada Zingarini, Giovanni Poggi, Koki Nagano, and Luisa Verdoliva. On the detection of synthetic images generated by diffusion models. In *ICASSP 2023-2023 IEEE International Conference on Acoustics, Speech and Signal Processing (ICASSP)*, pages 1–5. IEEE, 2023. 2
- [12] Davide Cozzolino, Giovanni Poggi, Riccardo Corvi, Matthias Nießner, and Luisa Verdoliva. Raising the bar of ai-generated image detection with clip. In *Proceedings of the IEEE/CVF Conference on Computer Vision and Pattern Recognition*, pages 4356–4366, 2024. 3
- [13] Prafulla Dhariwal and Alexander Nichol. Diffusion models beat gans on image synthesis. *Advances in neural information processing systems*, 34:8780–8794, 2021. 7
- [14] Tarik Dzanic, Karan Shah, and Freddie Witherden. Fourier spectrum discrepancies in deep network generated images. *Advances in neural information processing systems*, 33:3022–3032, 2020. 2
- [15] Patrick Esser, Sumith Kulal, Andreas Blattmann, Rahim Entezari, Jonas Müller, Harry Saini, Yam Levi, Dominik Lorenz, Axel Sauer, Frederic Boesel, et al. Scaling rectified flow transformers for high-resolution image synthesis. In *Forty-first international conference on machine learning*, 2024. 7
- [16] Joel Frank, Thorsten Eisenhofer, Lea Schönherr, Asja Fischer, Dorothea Kolossa, and Thorsten Holz. Leveraging frequency analysis for deep fake image recognition. In *International conference on machine learning*, pages 3247–3258. PMLR, 2020. 2
- [17] Shuyang Gu, Dong Chen, Jianmin Bao, Fang Wen, Bo Zhang, Dongdong Chen, Lu Yuan, and Baining Guo. Vector quantized diffusion model for text-to-image synthesis. In *Proceedings of the IEEE/CVF conference on computer vision and pattern recognition*, pages 10696–10706, 2022. 7
- [18] Fabrizio Guillaro, Giada Zingarini, Ben Usman, Avneesh Sud, Davide Cozzolino, and Luisa Verdoliva. A bias-free training paradigm for more general ai-generated image detection. In *Proceedings of the Computer Vision and Pattern Recognition Conference*, pages 18685–18694, 2025. 3
- [19] Seoyeon Gye, Junwon Ko, Hyounguk Shon, Minchan Kwon, and Junmo Kim. Reducing the content bias for ai-generated image detection. In *2025 IEEE/CVF Winter Conference on Applications of Computer Vision (WACV)*, pages 399–408. IEEE, 2025. 3
- [20] Jian Han, Jinlai Liu, Yi Jiang, Bin Yan, Yuqi Zhang, Zehuan Yuan, Bingyue Peng, and Xiaobing Liu. Infinity: Scaling bit-wise autoregressive modeling for high-resolution image synthesis. In *Proceedings of the Computer Vision and Pattern Recognition Conference*, pages 15733–15744, 2025. 7
- [21] Zexi Jia, Chuanwei Huang, Yeshuang Zhu, Hongyan Fei, Xiaoyue Duan, Zhiqiang Yuan, Ying Deng, Jiawei Zhang, Jinchao Zhang, and Jie Zhou. Secret lies in color: Enhancing ai-generated images detection with color distribution analysis. In *Proceedings of the Computer Vision and Pattern Recognition Conference*, pages 13445–13454, 2025. 2, 7
- [22] Tero Karras, Timo Aila, Samuli Laine, and Jaakko Lehtinen. Progressive growing of gans for improved quality, stability, and variation. In *International Conference on Learning Representations*, 2018. 6

- [23] Tero Karras, Samuli Laine, and Timo Aila. A style-based generator architecture for generative adversarial networks. In *Proceedings of the IEEE/CVF conference on computer vision and pattern recognition*, pages 4401–4410, 2019. 6
- [24] Sohail Ahmed Khan and Duc-Tien Dang-Nguyen. Clipping the deception: Adapting vision-language models for universal deepfake detection. In *Proceedings of the 2024 International Conference on Multimedia Retrieval*, pages 1006–1015, 2024. 3, 7
- [25] Bo Liu, Fan Yang, Xiuli Bi, Bin Xiao, Weisheng Li, and Xinbo Gao. Detecting generated images by real images. In *European Conference on Computer Vision*, pages 95–110. Springer, 2022. 2, 7
- [26] Yunpeng Luo, Junlong Du, Ke Yan, and Shouhong Ding. Lare²: Latent reconstruction error based method for diffusion-generated image detection. In *Proceedings of the IEEE/CVF Conference on Computer Vision and Pattern Recognition*, pages 17006–17015, 2024. 2
- [27] Alexander Quinn Nichol, Prafulla Dhariwal, Aditya Ramesh, Pranav Shyam, Pamela Mishkin, Bob McGrew, Ilya Sutskever, and Mark Chen. Glide: Towards photorealistic image generation and editing with text-guided diffusion models. In *International Conference on Machine Learning*, pages 16784–16804. PMLR, 2022. 7
- [28] Utkarsh Ojha, Yuheng Li, and Yong Jae Lee. Towards universal fake image detectors that generalize across generative models. In *Proceedings of the IEEE/CVF Conference on Computer Vision and Pattern Recognition*, pages 24480–24489, 2023. 3, 6, 7
- [29] Taesung Park, Ming-Yu Liu, Ting-Chun Wang, and Jun-Yan Zhu. Semantic image synthesis with spatially-adaptive normalization. In *Proceedings of the IEEE/CVF conference on computer vision and pattern recognition*, pages 2337–2346, 2019. 6
- [30] Alec Radford, Jong Wook Kim, Chris Hallacy, Aditya Ramesh, Gabriel Goh, Sandhini Agarwal, Girish Sastry, Amanda Askell, Pamela Mishkin, Jack Clark, et al. Learning transferable visual models from natural language supervision. In *International conference on machine learning*, pages 8748–8763. PMLR, 2021. 3
- [31] Aditya Ramesh, Mikhail Pavlov, Gabriel Goh, Scott Gray, Chelsea Voss, Alec Radford, Mark Chen, and Ilya Sutskever. Zero-shot text-to-image generation. In *International conference on machine learning*, pages 8821–8831. Pmlr, 2021. 7
- [32] Jonas Ricker, Denis Lukovnikov, and Asja Fischer. Aeroblade: Training-free detection of latent diffusion images using autoencoder reconstruction error. In *Proceedings of the IEEE/CVF Conference on Computer Vision and Pattern Recognition*, pages 9130–9140, 2024. 2
- [33] Robin Rombach, Andreas Blattmann, Dominik Lorenz, Patrick Esser, and Björn Ommer. High-resolution image synthesis with latent diffusion models. In *Proceedings of the IEEE/CVF conference on computer vision and pattern recognition*, pages 10684–10695, 2022. 7
- [34] Andreas Rossler, Davide Cozzolino, Luisa Verdoliva, Christian Riess, Justus Thies, and Matthias Nießner. Faceforensics++: Learning to detect manipulated facial images. In *Proceedings of the IEEE/CVF international conference on computer vision*, pages 1–11, 2019. 6
- [35] Peize Sun, Yi Jiang, Shoufa Chen, Shilong Zhang, Bingyue Peng, Ping Luo, and Zehuan Yuan. Autoregressive model beats diffusion: Llama for scalable image generation. *arXiv preprint arXiv:2406.06525*, 2024. 7
- [36] Chuangchuang Tan, Yao Zhao, Shikui Wei, Guanghua Gu, and Yunchao Wei. Learning on gradients: Generalized artifacts representation for gan-generated images detection. In *Proceedings of the IEEE/CVF Conference on Computer Vision and Pattern Recognition*, pages 12105–12114, 2023. 2
- [37] Chuangchuang Tan, Yao Zhao, Shikui Wei, Guanghua Gu, Ping Liu, and Yunchao Wei. Rethinking the up-sampling operations in cnn-based generative network for generalizable deepfake detection. In *Proceedings of the IEEE/CVF Conference on Computer Vision and Pattern Recognition*, pages 28130–28139, 2024. 2, 7
- [38] Keyu Tian, Yi Jiang, Zehuan Yuan, Bingyue Peng, and Liwei Wang. Visual autoregressive modeling: Scalable image generation via next-scale prediction. *Advances in neural information processing systems*, 37:84839–84865, 2024. 7
- [39] Sheng-Yu Wang, Oliver Wang, Richard Zhang, Andrew Owens, and Alexei A Efros. Cnn-generated images are surprisingly easy to spot... for now. In *Proceedings of the IEEE/CVF conference on computer vision and pattern recognition*, pages 8695–8704, 2020. 2, 7
- [40] Zhendong Wang, Jianmin Bao, Wengang Zhou, Weilun Wang, Hezhen Hu, Hong Chen, and Houqiang Li. Dire for diffusion-generated image detection. In *Proceedings of the IEEE/CVF International Conference on Computer Vision*, pages 22445–22455, 2023. 2
- [41] Shiyu Wu, Jing Liu, Jing Li, and Yequan Wang. Few-shot learner generalizes across ai-generated image detection. In *Forty-second International Conference on Machine Learning*, 2025. 3
- [42] Jinheng Xie, Weijia Mao, Zechen Bai, David Junhao Zhang, Weihao Wang, Kevin Qinghong Lin, Yuchao Gu, Zhijie Chen, Zhenheng Yang, and Mike Zheng Shou. Show-o: One single transformer to unify multimodal understanding and generation. In *The Thirteenth International Conference on Learning Representations*, 2024. 7
- [43] Zhiyuan Yan, Jiangming Wang, Peng Jin, Ke-Yue Zhang, Chengchun Liu, Shen Chen, Taiping Yao, Shouhong Ding, Baoyuan Wu, and Li Yuan. Orthogonal subspace decomposition for generalizable ai-generated image detection. In *Forty-second International Conference on Machine Learning*, 2025. 3
- [44] Haifeng Zhang, Qinghui He, Xiuli Bi, Weisheng Li, Bo Liu, and Bin Xiao. Towards universal ai-generated image detection by variational information bottleneck network. In *Proceedings of the Computer Vision and Pattern Recognition Conference*, pages 23828–23837, 2025. 3, 7
- [45] Kaiyang Zhou, Jingkang Yang, Chen Change Loy, and Ziwei Liu. Learning to prompt for vision-language models. *International Journal of Computer Vision*, 130(9):2337–2348, 2022. 5
- [46] Ziyin Zhou, Yunpeng Luo, Yuanchen Wu, Ke Sun, Jiayi Ji, Ke Yan, Shouhong Ding, Xiaoshuai Sun, Yunsheng Wu, and

Rongrong Ji. Aigi-holmes: Towards explainable and generalizable ai-generated image detection via multimodal large language models. *arXiv preprint arXiv:2507.02664*, 2025. [6](#)

- [47] Jun-Yan Zhu, Taesung Park, Phillip Isola, and Alexei A Efros. Unpaired image-to-image translation using cycle-consistent adversarial networks. In *Proceedings of the IEEE international conference on computer vision*, pages 2223–2232, 2017. [6](#)
- [48] Mingjian Zhu, Hanting Chen, Qiangyu Yan, Xudong Huang, Guanyu Lin, Wei Li, Zhijun Tu, Hailin Hu, Jie Hu, and Yunhe Wang. Genimage: A million-scale benchmark for detecting ai-generated image. *Advances in Neural Information Processing Systems*, 36, 2024. [6](#)